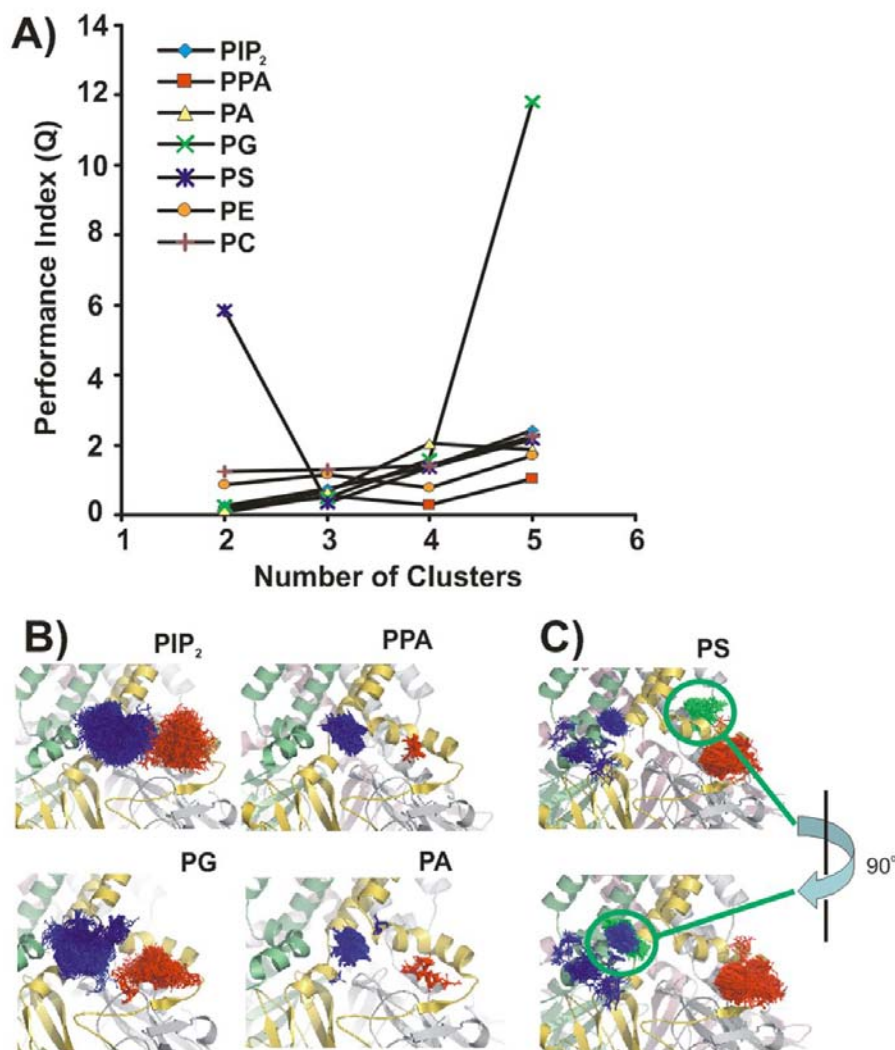


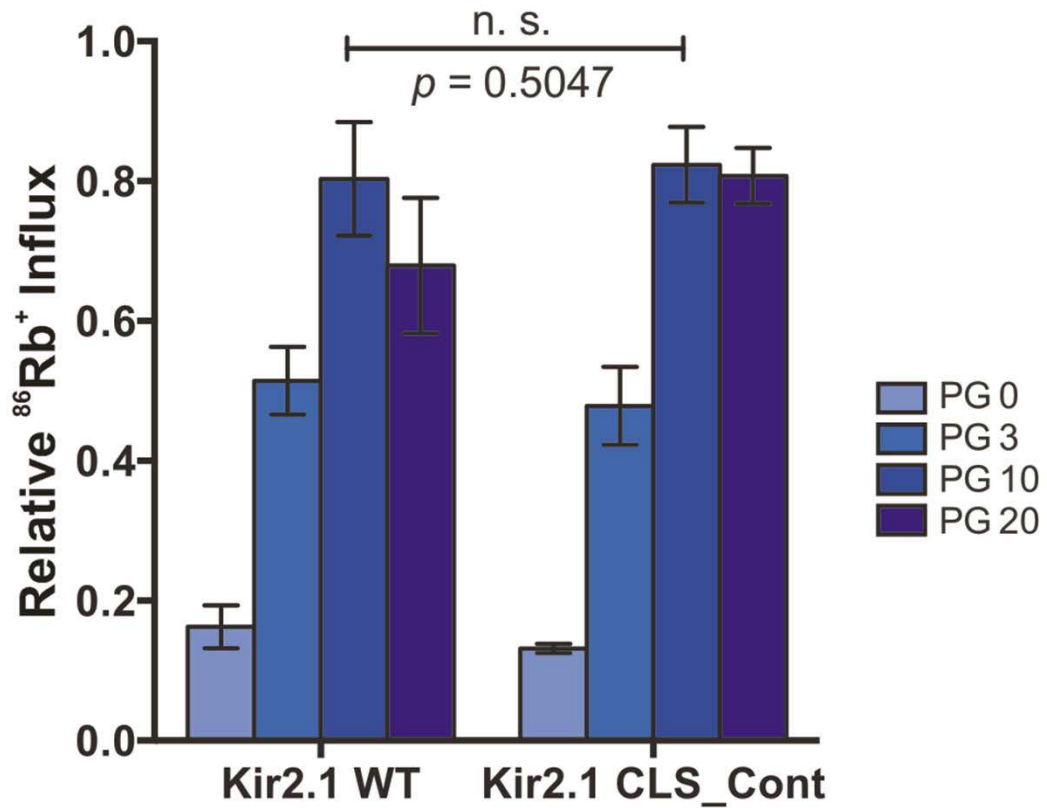
### Supplementary Figure S1. Head group charge

The PIP<sub>2</sub> head group charges were obtained from the report and the charge of PPA was generated and generously provided by the Lim group in University of Kansas City. Both were adjusted to be compatible with the precedent CHARMM force field parameters. The charges of the remaining lipids were directly taken from the CHARMM force field parameters. A dotted arrow for each lipid designated the molecular vector. The angle between the molecular vector and membrane outward normal vector was used to determine the relative orientation of lipid head groups to the membrane. If the angle between the two vectors was greater than 90°, the head group was pointing toward the membrane and rejected. Phosphatidic acid was excluded for the head group orientation test since due to its small head group it has more flexibility in their head group orientation. Charge of each atom is shown while the charges of equivalent atoms are not shown for clarity. The total charge of each head group is shown in a bracket.



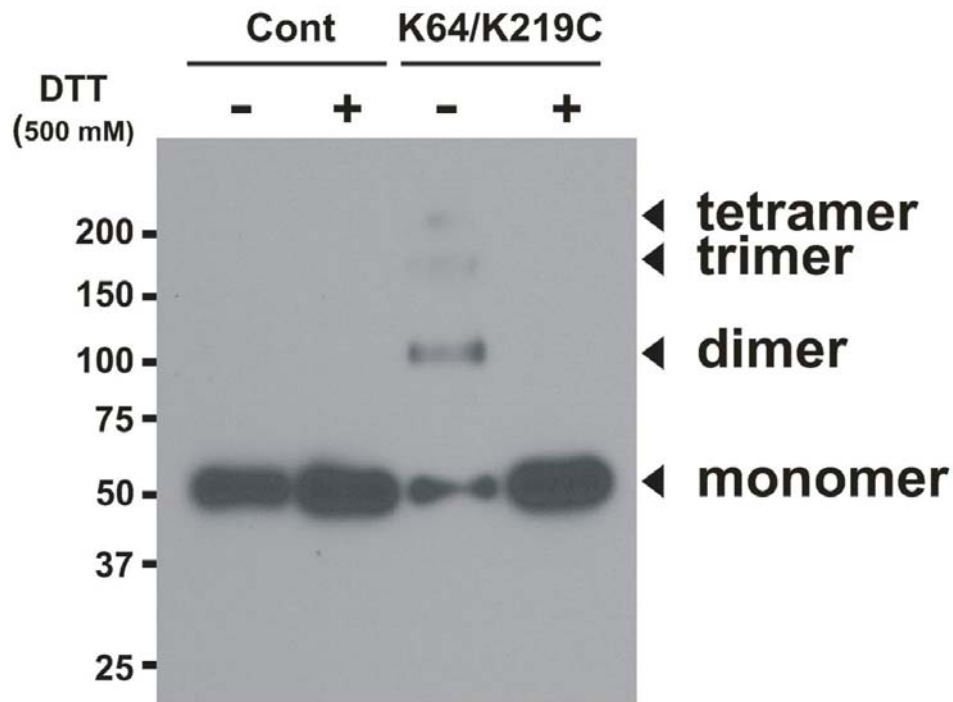
### Supplementary Figure S2. Performance index to evaluate clustering

A) Performance index(Q) B) All the accepted poses of negatively charged lipids clustered into either the Primary (blue) or the Secondary (red) site. C) The three clusters of PS are shown in blue (primary), red (secondary) and green (third) clusters (top). The poses of the third cluster were rotated by 90 ° along the pore axis (bottom). In order to cluster all the accepted poses, the position of the phosphate atom directly connected to the glycerol moiety in a ligand was used as a metric. K-mean clustering and performance index calculation was performed in the same manner as described previously. A trial of clustering into 2 to 5 clusters was repeated for 5 times and performance index was computed each time. Shown in the figure is the list of performance index of a clustering trial where the minimum performance index was generated. Except for PS, all lipids showed the minimum value with 2 clusters. PS was the only exception with three apparent clusters. However, the third cluster is in the same location as cluster 1 at the neighboring subunit interface, a region of the protein that was partly included in the search space. This additional binding was likely facilitated for PS but none of the other lipids because PS alone adopted certain poses as a result of the zwitterionic headgroup.



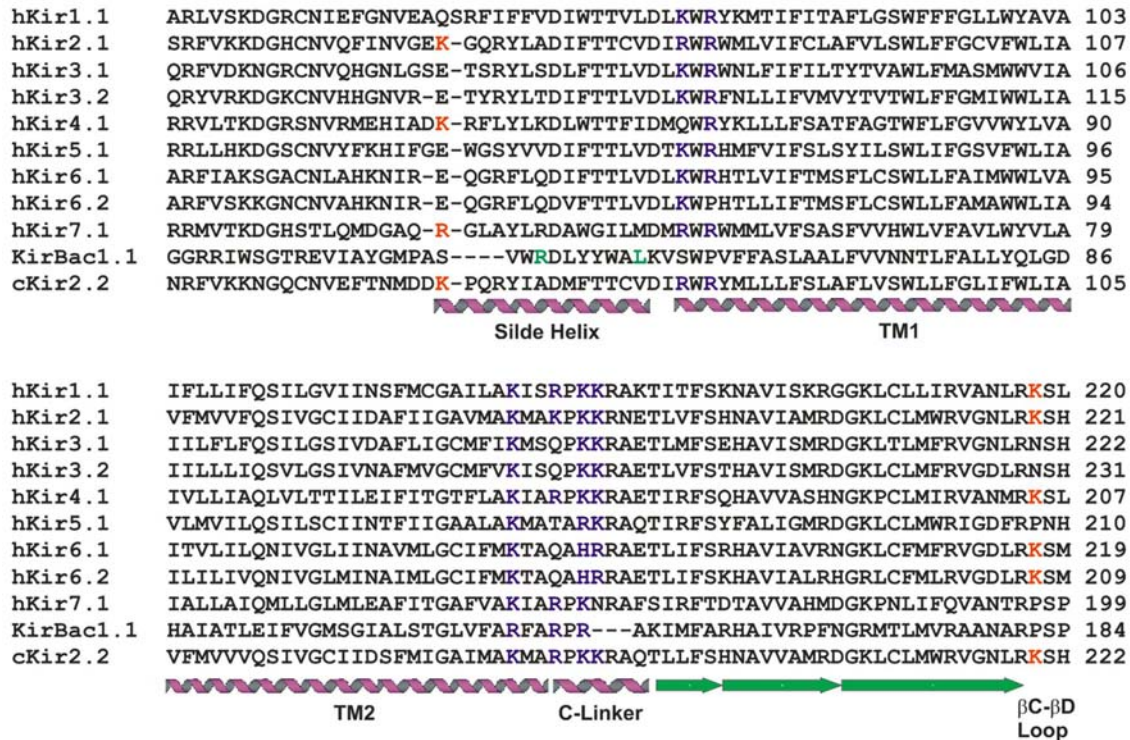
**Supplementary Figure S3. CLS\_Cont is functionally equivalent to Kir2.1 wild type proteins.**

PL(-) dependent CLS\_Cont activity was compared to that of Kir2.1 wild type protein. Channel activity was measured in the proteoliposomes made of constant 0.1 % PIP<sub>2</sub> and increasing amount of POPG (zero, 3, 10, and 20 %). Channel activities of the two proteins are not statistically different when tested by two-way ANOVA (mean  $\pm$  s.d., n=3 replicates).



**Supplementary Figure S4. Disulfide bond formation between K64C and K219C in the double mutant**

Kir2.1 CLS-Cont and Kir2.1 CLS\_K64/K219C double mutant proteins were purified from yeast cells, quantified using absorbance at 280 nm, and 10 ng of proteins were loaded into SDS-acrylamide gel without or with 500 mM dithiothreitol (DTT). Proteins were transferred to a PVDF membrane and visualized by anti-FLAG monoclonal antibody and chemiluminescent substrate. Dimeric bands are prominent only in the double mutant protein, and sensitive to reduction by DTT, consistent with a disulfide bond between K64C and K219C that stabilizes multimeric forms of the double mutant in oxidizing conditions.



### Supplementary Figure S5. Sequence alignment of Kir subfamilies.

Shown are aligned sequences of Kir subfamilies for the parts of interest in this study. Residues relevant to PIP<sub>2</sub> binding are shown in purple. Residues for the secondary PL(-) effect are shown in red. The secondary structure and conventional name for parts of sequences are designated below. In particular, 35R of hKir7.1 alignment to K64 of Kir2.1 depends on the combinations of sequences for multiple alignments.



Apo-Docking								
Subunit	Residue	PIP2	PPA	PA	PG	PS	PE	PC
A	H53	0.032	0.000	0.000	0.011	0.000	0.010	0.000
	Q57	0.274	0.000	0.662	0.199	0.028	0.164	0.044
	F58	0.000	0.000	0.014	0.053	0.183	0.404	0.000
	D60	0.000	0.000	0.000	0.007	0.308	0.000	0.000
	V61	0.006	0.000	0.006	0.042	0.362	0.010	0.000
	G62	0.000	0.000	0.000	0.009	0.212	0.000	0.000
	K64	1.369	1.000	1.077	1.059	0.858	0.577	0.933
	Y68	0.000	0.000	0.063	0.127	0.000	0.000	0.000
B	R218	0.000	0.000	0.000	0.314	0.000	0.048	0.000
	K219	1.643	1.497	1.404	1.499	0.270	1.058	0.911
	S220	0.000	0.000	0.000	0.276	0.000	0.010	0.000
	K338	0.006	0.000	0.000	0.001	0.138	0.000	0.000

PIP <sub>2</sub> -bound-Docking								
Subunit	Residue	PIP2	PPA	PA	PG	PS	PE	PC
A	H53	0.016	0.003	0.002	0.035	0.002	0.046	0.104
	Q57	0.331	0.175	0.142	0.206	0.142	0.176	0.195
	F58	0.019	0.009	0.126	0.050	0.126	0.287	0.000
	D60	0.040	0.002	0.057	0.028	0.057	0.003	0.002
	V61	0.062	0.003	0.061	0.095	0.061	0.018	0.011
	G62	0.013	0.002	0.000	0.029	0.000	0.001	0.002
	K64	1.422	1.137	1.170	1.074	1.170	0.638	0.816
	Y68	0.000	0.000	0.000	0.131	0.016	0.000	0.000
B	R218	0.000	0.010	0.106	0.286	0.106	0.052	0.013
	K219	1.331	1.472	1.022	1.197	1.022	0.957	0.875
	S220	0.000	0.000	0.121	0.185	0.121	0.008	0.012
	K338	0.115	0.000	0.087	0.001	0.087	0.000	0.000

**Supplementary Table S1. Hydrogen bonding frequency between docked poses and residues at Secondary site.**

The exact number of hydrogen bonding frequency is shown for the Apo- and Holo-docking. The residue and lipid pairs of the frequency greater than 1 are marked in yellow.